2014 IEEE International Conference on Robotics & Automation (ICRA)
Hong Kong Convention and Exhibition Center
May 31 - June 7, 2014. Hong Kong, China

Rendering Viscoelasticity with Series Elastic Actuators using Cascade Control

Nevio Luigi Tagliamonte*, Dino Accoto and Eugenio Guglielmelli

Abstract— **Rotary Series Elastic Actuators (SEAs) are largely adopted to safely and accurately modulate interaction torques when robots operate in close contact with humans. Torque control is often based on a cascade scheme including PI regulators for a velocity controller nested in a torque controller. This solution is simple, robust and can potentially guarantee coupled stability. A high-level impedance control loop is also commonly added to regulate the behavior of the interaction port as a desired virtual viscoelastic body. In the present work, passivity is analyzed when a cascade controlled SEA is employed to display a virtual parallel spring-damper system. The case of a null desired impedance and of a pure spring are also tackled. The range of renderable mechanical impedance and guidelines for the selection of the control gains are derived.**

I. Introduction

When robots interact with the environment and/or with the human body, compliant actuators [1] and interaction control schemes [2] are typically used, thus overcoming adaptability and safety limits of stiff gearmotors and position controllers.

To accurately and stably modulate human-robot interaction, actuators operating in torque control mode are required. An ideal torque source is capable of perfect torque tracking and has null mechanical impedance (defined as the transfer function between the output torque and the input angular velocity in response to which the torque is generated). Rotary Series Elastic Actuators (SEAs) [3], approximate these characteristics since a spring is serially connected to a gearmotor to intrinsically reduce the output impedance and to implement torque control (the measurement of the spring deflection, considering known torque-angle characteristic, allows obtaining a torque feedback signal). The introduction of series elasticity also ensures tolerance to impacts and rejection of disturbances (at high frequencies the impedance reduces to the one of the spring), protection of motor/gearbox from damages due to accidental collisions, minimization of stiction, friction and backlash, and energy storage. Series compliance allows increasing torque control gains and reducing intrinsic impedance but it lowers the achievable control bandwidth with respect to high-impedance actuators [4]. Hence, the selection of the spring stiffness is crucial and also practical design can be quite challenging [5]. Performance degradation, increasing with compliance and with delivered torques, is often recovered by using elastic elements whose stiffness can be varied during operation [1] or pre-set according to a specific task [6]. A number of rotary SEA prototypes have been recently developed [7]–[12] and are often employed in assistance and rehabilitation robotics [7], [8], [13]. In these applications, machines operate compliantly to prevent the transfer of harmful forces to the human limbs and complement user's motion with the minimum amount of assistance. To this aim, impedance control [2] is typically implemented on top of torque control: robot behaves, in Cartesian or joint space, as a virtual viscoelastic system around a desired equilibrium trajectory.

Different approaches to SEA torque/impedance control have been proposed. First solutions entailed PID regulation of motor current with feedforward compensation of motor inertia [3]. A proper selection of the feedforward term and the substitution of the integrator with a low-pass filter allowed stability during interaction with passive systems. To use the motor as a velocity generator, in [9] a PI velocity loop was nested in a PI torque control loop. The same cascade scheme was proposed in [14] and in [15], where passivity conditions for the torque control and for a high-level stiffness control were also derived. In [12] torque regulation was based on a PD controller and on a disturbance observer, capable of compensating model errors and plant variations. A similar model-based solution was presented in [16]. Ultimately, torque/impedance control based on cascade scheme with low-level velocity regulation is the most widely used solution [9]–[11], [15], because of robustness, ease of tuning and the potential of guaranteeing passivity, all while still counteracting static errors.

The objective of this paper is to analyze passivity for SEAs when cascade control approach is employed and impedance regulation is implemented to render a linear viscoelastic behavior in the form of a parallal spring-damper system. Hints on the use of the cascade control and guidelines for gains selection will be reported. The work extends the results on pure virtual elasticity presented in [15].

II. System modelling and problem definition

A. SEA model and control

The block scheme of the SEA control considered in this work is reported in Fig. 1. SEA model includes inertia J_a, viscous friction c_a, and series elasticity k_s. The symbols τ_m and θ_m represent motor torque and rotation. A PI controller (proportional and integral gains: P_v and I_v) is used in the inner *velocity* control loop and a second PI controller is used for the outer *torque* control loop (proportional and integral gains: P_t and I_t). Given a linear torque-deflection relationship for the spring, the feedback signal for the torque controller, *i.e.* the torque delivered by the actuator, can be calculated as $\tau =$

The Authors are with Università Campus Bio-Medico di Roma, Laboratory of Biomedical Robotics and Biomicrosystems, Center of Integrated Research (CIR), Via Álvaro del Portillo, 21 - 00128 Rome, Italy.
*Corresponding author: n.tagliamonte@unicampus.it

978-1-4799-3684-7/14/$31.00 ©2014 IEEE

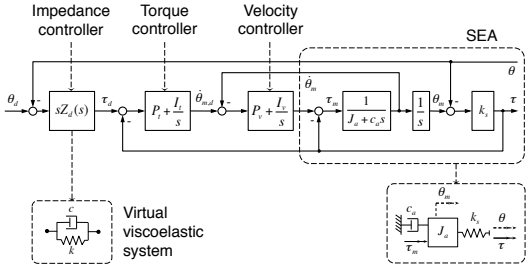

Fig. 1. Block scheme of the SEA cascade control.

$k_s(\theta - \theta_m)$, being θ the SEA output rotation. An impedance controller generates viscoelastic torques τ_d as set-point for the torque controller according to the desired impedance $Z_d(s)$ to be virtually rendered around the equilibrium position θ_d. In turn, the torque controller generates the set-point $\dot{\theta}_{m,d}$ for the velocity controller.

Some design-specific characteristics (depending on the practical device implementations) have been neglected to preserve the generality of the analysis. In particular, the following assumptions have been considered: *i)* Nonlinear friction and backlash are neglected, so that linearity of the model is assured. *ii)* Electric components, that introduce high-frequency contributions, are ignored. *iii)* The overall inertia and viscous friction of the actuator are considered on the motor side and, for simplicity sake, the reduction ratio due to gearbox is not explicitly represented. *iv)* Motor velocity signal has negligible delay. This simplification is acceptable since encoders with high sampling frequency and low quantization are typically used in SEAs and differentiation filters act at frequencies far outside the bandwidth of interest; nonetheless, several methods for the encoder-based estimation of velocity with zero/small delay can be employed (*e.g.* polynomial fitting, Kalman filtering, nonlinear estimators [17]). *v)* As it will be described later on (Sec. II-B), the effect of load inertia can be neglected for the purpose of this study. *vi)* For the sake of simplicity, a null desired angle is assumed for the impedance controller. *vii)* Saturation effects are not directly taken into account: conditions for the selection of the controller gains will be reported, provided that motor limitations are considered in practical implementations.

Despite these simplifications, the model is able to catch the main features of SEA cascade control and can be used to analyze actuator performance and to design the controller. Nonetheless, similar approaches were pursued in other works on SEAs modelling and control [4], [9], [14], [15].

B. Coupled stability and passivity

Foundational studies on direct force control analyzed instability during the interaction between a manipulator and the environment [18], [19]. In [19] it was shown that a stable robot (*isolated stability*) can exhibit instability during interactions (*coupled instability*). The analysis on a simplified linear system showed that, if a force controlled plant has the interaction port of a *passive* system, then coupled stability is ensured during the interaction with any arbitrary passive environments. It would appear that this passivity criterion cannot be applied to guarantee stability during human-robot interaction since the human motor system is basically non-passive. Anyhow, because of the limited human motion power and frequency content and of the low human body mechanical impedance, passivity-based controllers can be still considered a suitable safety solution [18], [19], even though sometimes exceedingly conservative, according to empirical demonstrations [20], [21].

Passivity for the cascade controlled SEA is ensured if its impedance transfer function $Z(s)$ is positive real [19]. This is verified *iff*:

1) $Z(s)$ has no poles in the right half plane and any imaginary pole is simple.
2) $\mathrm{Re}\{Z(j\omega)\}$ is nonnegative for all $\omega \in (-\infty, +\infty)$ for which $j\omega$ is not a pole of $Z(s)$.

Passivity can be also easily checked in the Bode plot of the frequency response $Z(j\omega)$ by verifying that the phase remains within the interval ± 90 deg. It is also worth noticing that the impedance of the system, when an inertial load J_l is added, can be calculated as $Z^{Z,l}(s) = Z(s) + sJ_l$. Since $\mathrm{Re}\{Z(j\omega)\} = \mathrm{Re}\{Z^{Z,l}(j\omega)\}$, passivity does not depend on the presence of the inertial load.

Conservative passivity conditions for a torque controlled SEA were deduced in [14] while the addition of an outer impedance control loop to render a virtual spring was analyzed in [15]. Here previous results will be extended by considering viscous friction in the actuator model and by investigating the case where the impedance transfer function of a linear viscoelastic model in the form of a parallel spring-damper system has to be rendered.

III. Passivity for the Cascade Control

In this section passivity conditions for the haptic rendering of generic impedance transfer functions will be deduced while in the following section they will be adapted to the case of a parallel spring-damper system. The specific cases of a pure spring and of null impedance (ideal backdrivability) will be also analyzed.

Considering a desired virtual impedance in the form $Z_d(s) = N_{Z_d}(s)/D_{Z_d}(s)$, the impedance transfer function of the controlled SEA is

$$Z(s) = k_s \frac{\sum_{i=0}^{3} n_i s^i}{D_{Z_d}(s) D_Z(s)} := \frac{N'_Z(s)}{D'_Z(s)}, \tag{1}$$

with $n_0 = N_{Z_d}(s) I_t I_v$, $n_1 = D_{Z_d}(s) I_v + N_{Z_d}(s)(I_t P_v + I_v P_t)$, $n_2 = D_{Z_d}(s)(P_v + c_a) + N_{Z_d}(s) P_t P_v$, $n_2 = D_{Z_d}(s)(P_v + c_a) + N_{Z_d}(s) P_t P_v$, $n_3 = D_{Z_d}(s) J_a$ and being

$$\begin{aligned} D_Z(s) &= J_a s^4 + (P_v + c_a) s^3 + (k_s + I_v + P_t P_v k_s) s^2 + \\ &+ (I_t P_v + I_v P_t) k_s s + I_t I_v k_s \end{aligned} \tag{2}$$

the same characteristic polynomial of the closed-loop torque control transfer function. From (1) it can be noticed that the first passivity condition reported in Sec. II-B is satisfied if

torque controlled SEA is stable and if $D_{Z_d}(s)$ only introduces in $Z(s)$ poles with negative real part or simple imaginary poles. To verify stability condition, Hurwitz determinants $\Delta_h(s)$ $(h=1,\ldots,3)$ can be calculated based on (2), as

$$\begin{aligned}\Delta_1(s) &= J_a^{-1}\,(P_v+c_a)\\ \Delta_2(s) &= J_a^{-2}\,[(P_v+c_a)\,(I_v+k_s)+k_s\,p]\\ \Delta_3(s) &= J_a^{-1}\,\Delta_2(s)\,(\mu+\nu)\,P_t\,P_v-J_a^{-3}I_t\,I_v\,(P_v+c_a)^2\end{aligned} \tag{3}$$

with $p=P_t\,P_v\,[P_v+c_a-J_a\,(\mu+\nu)]$, $I_v=\mu\,P_v$ and $I_t=\nu\,P_t$.

Since $J_a>0$, $P_v>0$ and $c_a>0$, it derives that $\Delta_1(s)>0$. Moreover, conservative conditions to assure that $\Delta_2(s)$ and $\Delta_3(s)$ are positive are

$$\left\{\begin{array}{lcl} P_v &>& J_a\,(\mu+\nu)-c_a\\ I_v &>& \nu\,c_a\end{array}\right. \tag{4}$$

which generalize the result found in [14], [15], where it was suggested to select P_v greater than J_a and both integrator gains as half of the relative proportional gains. Conditions (4) allow a more flexible choice of integrator gains, which is a quite important aspect, especially in counteracting static errors and in displaying null impedance, as it will be shown later on. It can be also added that, the second condition in (4) is automatically satisfied if $\mu>\frac{c_a}{J_a}$. Moreover, in practical implementations, selected gains not only have to satisfy the presented constraints, but also have to be compatible with motor limitations due to torque and velocity saturation.

The positiveness of $\mathrm{Re}\{Z(j\omega)\}$ is verified if

$$\begin{aligned}P(\omega) &= \mathrm{Re}\left\{N_Z'(j\omega)\right\}\mathrm{Re}\left\{D_Z'(j\omega)\right\}+\\ &+ \mathrm{Im}\left\{N_Z'(j\omega)\right\}\mathrm{Im}\left\{D_Z'(j\omega)\right\}=\\ &= \textstyle\sum_{i=1}^{r} d_i\,\omega^i>0\end{aligned} \tag{5}$$

depending r, the order of the polynomial in ω, on the specific frequency response. The polynomial $P(\omega)$ is nonnegative for all $\omega\in(-\infty,+\infty)$ if all coefficients d_i are nonnegative.

IV. Virtual parallel spring-damper system

One of the most commonly used control schemes during human-robot interaction consists in the haptic rendering of viscoelasticity in the form of a parallel spring-damper system (Fig. 1). In other words, the sum of elastic and viscous torques is transferred to the human body. Passivity when cascade approach is adopted for SEA control is analyzed here. In what follows, only positive values of the virtual stiffness k and of the damping coefficient c (the most common case in real applications) will be considered. Numerical quantities reported in Tab. I will be used for demonstration purposes. Actuator data are representative of typical implementations including electric motors with power in the range 300–600 W [7], [8], [11].

If the desired virtual impedance in the controller of Fig. 1 consists of a spring and a damper connected in parallel, its transfer function is

$$Z_d^{sd}(s)=\frac{k+c\,s}{s} \tag{6}$$

TABLE I

Numerical values for model parameters.

Mechanical parameters		
J_a	0.15	kg m^2
c_a	3	N m s/rad
k_s	250	N m/rad

Control gains		
P_v	4	N m s/rad
I_v	1.6	N m/rad
P_t	0.8	rad/(s N m)
I_t	0.24	rad/(s^2 N m)

and (1) becomes

$$Z^{sd}(s)=k_s\,\frac{\sum_{i=0}^{4} n_i^{sd}\,s^i}{s\,D_Z(s)} \tag{7}$$

with $n_0^{sd}=I_t\,I_v\,k$, $n_1^{sd}=I_t\,I_v\,c+(\mu+\nu)\,k$, $n_2^{sd}=I_v+P_t\,P_v\,[(\mu+\nu)\,c+k]$, $n_3^{sd}=P_v+c_a+P_t\,P_v\,c$ and $n_3^{sd}=J_a$.

No other poles than one at the origin are added to the denominator of the overall impedance transfer function $Z(s)$, hence the first condition on passivity in Sec. II-B is not violated. Non null coefficients of $P^{sd}(\omega)$ are

$$\begin{aligned}d_2^{sd}(c) &= {k_s}^2\,{I_t}^2\,{I_v}^2\,c\\ d_4^{sd}(k,c) &= k_s\,[(k_s-k)\,q-k_s\,k\,(\mu+\nu)\,P_t\,P_v+c\,h_1]\\ d_6^{sd}(k,c) &= k_s\,[(k_s-k)\,p+(P_v+c_a)\,k_s+c\,h_2]\\ d_8^{sd}(c) &= -J_a\,P_t\,P_v\,k_s\,c\end{aligned} \tag{8}$$

with $q=I_v(I_v P_t-I_t\,c_a)$, $h_1=k_s\left(\mu^2+\nu^2\right)P_t^2\,P_v^2-I_t\,I_v\,(k_s+I_v)$, and $h_2=P_t\,P_v\,[(P_t\,P_v+1)\,k_s-(\mu+\nu)\,c_a]+I_t\left(I_v\,J_a-P_v^2\right)$.

For $c\in(0,\infty)$, $d_2^{sd}>0$ and $d_8^{sd}<0$. The coefficient d_8^{sd} being negative, passivity constraint cannot be satisfied. In Fig. 2 the frequency response $Z^{sd}(j\omega)$ is reported by representatively considering $k=100$ N m/rad and $c=10$ N m s/rad (and consequently cut-off frequency $\omega^{sd}=k/c=10$ rad/s). It can be seen that, because of the lost of passivity, $|\angle Z^{sd}(j\omega)|>90$ deg. Since $P^{sd}(\omega)=P^{sd}(-\omega)$, $d_2^{sd}>0$ and $d_8^{sd}<0$, if $d_4^{sd}\geq 0$ and $d_6^{sd}\geq 0$, then the polynomial becomes negative after a frequency estimated as

$$\omega^{sd,p}(k,c)\approx\sqrt{d_6^{sd}/|d_8^{sd}|} \tag{9}$$

and passivity is lost.

The condition $d_4^{sd}\geq 0$ is satisfied if

$$k(c)\leq\tilde{k}^s+c\,\frac{h_1}{h_3}:=\tilde{k}^{sd,1}(c), \tag{10}$$

with

$$\tilde{k}^s=\frac{c_a-P_v\,\frac{\mu}{\nu}}{c_a-P_v\,\frac{\mu}{\nu}-k_s\,\frac{\mu+\nu}{\mu\,\nu}}<k_s \tag{11}$$

and $h_3=q+k_s\,(\mu+\nu)\,P_t\,P_v$.

In particular, if $\frac{h_1}{h_3}>0$, the maximum achievable virtual stiffness $\tilde{k}^{sd}$ is greater than $\tilde{k}^s$ and can be linearly increased with increasing c. Since $h_3>0$ when the second inequality in (4) is met, it is only required that $h_1>0$, *i.e.* that

$$P_t>\frac{\mu^2\,\nu}{k_s\,(\mu^2+\nu^2)}\left(1+\frac{k_s}{I_v}\right). \tag{12}$$

The condition $\frac{h_1}{h_3} > 0$, and in turn inequality (10), also conservatively assures that $\tilde{k}^{sd}(c) > 0$, thus avoiding that there exists a value $\bar{c} \mid \forall\, c \in (0,\bar{c}]$, $k(c) \leq 0$.

The condition $d_6^{sd} > 0$ is satisfied if

$$k(c) \leq \left(k_s + \frac{P_v + c_a}{p}\right) + c\,\frac{h_2}{p} := \tilde{k}^{sd,2}(c). \tag{13}$$

Since $p > 0$, because of (4), if $h_2 > 0$ (13) ensures that k can be linearly increased with increasing c. The condition $h_2 > 0$ is conservatively satisfied if

$$P_v > \frac{c_a\,\mu}{k_s P_t - \nu}, \tag{14}$$

which in turn is conservatively verified for $\nu < k_s P_t$ and $\mu < P_v/c$. Finally, from (10) and (13) it descends that for

$$c \in (0,\infty), \quad k \in \left(0, \tilde{k}^{sd,1}(c)\right] \cap \left(0, \tilde{k}^{sd,2}(c)\right]. \tag{15}$$

A. Particular cases: pure spring and zero impedance

1) Pure spring: The virtual rendering of a spring k is a specific case of the previous model, considering $c = 0$ in (6). This case was already discussed in [15] and here additional considerations on renderable stiffness will be provided, also analyzing the effect of viscous friction, which was previously neglected. The only non null coefficients of the polynomial $P^s(\omega)$ are $d_4^s(k) = d_4^{sd}(k,c)|_{c=0}$ and $d_6^s(k) = d_6^{sd}(k,c)|_{c=0}$. To assure that both coefficients are nonnegative, the following limitation on the achievable virtual stiffness is introduced:

$$k \leq \tilde{k}^s \tag{16}$$

being the condition $\tilde{k}^s = 0$ simply avoided thanks to (4).

As demonstrated in [15] the stiffness of the elastic element bounds the achievable virtual stiffness. In particular, (11) highlights the dependance of the maximum achievable stiffness $\tilde{k}^s$ not only from controller gains but also from the viscous friction. Anyhow, by substituting in (11) realistic values (see Tab. I) it can be verified that $\tilde{k}^s$ only slightly decreases with increasing c_a and is significantly lowered only

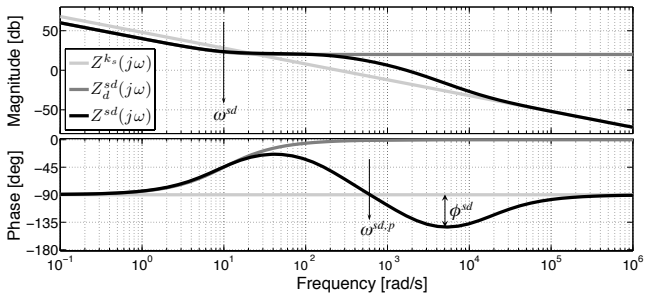

Fig. 2. Frequency response of the actuator impedance $Z^{sd}(j\omega)$ when rendering a virtual parallel spring-damper system ($Z_d^{sd}(j\omega) = (k + c\,j\omega)/j\omega$). Model parameters are $k = 100$ N m/rad and $c = 10$ N m s/rad ($\omega^{sd} = 10$ rad/s). The system is not passive since $\angle Z^{sd}(j\omega) < -90$ deg after a frequency $\omega^{sd,p}$. The maximum phase excess is ϕ^{sd}. At high frequencies the impedance approaches the one of the physical spring ($Z^{k_s}(j\omega)$).

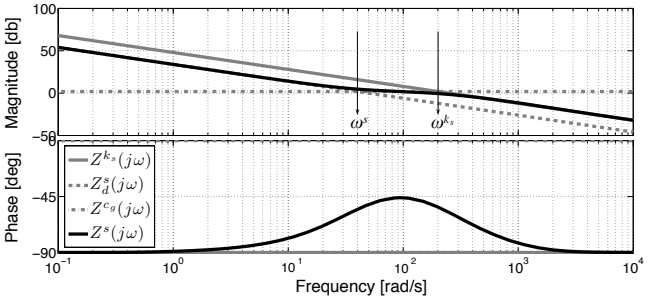

Fig. 3. Frequency response of the actuator impedance $Z^s(j\omega)$ when rendering pure virtual elasticity ($Z_d^s(j\omega) = k/j\omega$). For frequencies below ω^s the actuator behaves like a pure spring of stiffness $k = 50$ N m/rad as desired; for frequencies higher than ω^{k_s} the impedance reduces to the one of the physical spring ($Z^{k_s}(j\omega)$). For $\omega^s < \omega < \omega^{k_s}$ a damper, with damping coefficient c_g, is displayed ($Z^{c_g}(j\omega)$).

for values that are approximatively one order of magnitude higher than the nominal ones. Equations (11) and (16) show that high-stiffness behaviors cannot be rendered without a proper gains selection. Since $\lim_{P_t \to \infty} \tilde{k}^s = k_s\,\frac{I_v}{I_v + k_s}$, it is evident that the increase of P_t may not be sufficient to achieve a predefined level of stiffness and that also velocity gains may need to be modified. If a value $\bar{k} = \alpha k_s$ has to be passively rendered, the following inequality has to be considered:

$$I_v \geq \nu\,c_a + \frac{\alpha}{1-\alpha}\left(\frac{\mu + \nu}{\mu}\right) k_s. \tag{17}$$

The frequency response $Z^s(j\omega)$ is reported in Fig. 3 ($k = 50$ N m/rad is representatively set), which shows that the phase lies in the range ± 90 deg since system passivity is ensured by proper gains selection. For frequencies up to

$$\omega^s = \frac{k}{c_g} = \frac{k\,(1 + P_t P_v)}{P_v}, \tag{18}$$

the desired pure elastic behavior is successfully displayed. At intermediate frequencies a damper with damping coefficient

$$c_g := \frac{P_v}{1 + P_t P_v}, \tag{19}$$

only depending on the control gains, is rendered (frequency response: $Z^{c_g}(j\omega) = c_g$). For frequencies higher than

$$\omega^{k_s} = \frac{k_s}{c_g} = \frac{k_s\,(1 + P_t P_v)}{P_v}, \tag{20}$$

the impedance reduces to the one of the physical spring of stiffness k_s (frequency response: $Z^{k_s}(j\omega) = k_s/j\omega$).

If no integrators would have been employed, $\lim_{s \to 0} s Z^s(s)|_{\mu=\nu=0} = k\,\frac{P_t P_v}{1 + P_t P_v}$, thus for low frequencies the displayed stiffness would have been lower than the desired one, independently on the viscous friction.

2) Zero impedance: Commanding null impedance to the actuators of a robot is a possible method to make it be transparent to external actions. This can be considered as a particular case of (6), in which $k = c = 0$. The first passivity condition reported in Sec. II-B is again guaranteed by (4).

The only non null coefficients of the polynomial $P^z(\omega)$ are $d_4^z = d_4^{sd}(k,c)|_{k=c=0}$ and $d_6^z(k) = d_6^{sd}(k,c)|_{k=c=0}$, which are nonnegative if condition (4) is satisfied. It is worth noticing that both coefficients would have been automatically non-negative if no integrators were employed but the impedance, for all frequencies up to ω^{k_s}, would have reduced to the one of a pure damper with damping coefficient c_g, given by (19), which only depends on the chosen control gains.

For low frequencies

$$\lim_{s\to 0} \frac{Z^z(s)}{s} = \frac{1}{I^t} := J_g, \tag{21}$$

which shows that the SEA behaves as a pure equivalent inertia, whose value is inversely proportional to the torque control integral gain (frequency response: $Z^{J_g}(j\omega) = J_g\, j\omega$). For $\omega^z < \omega < \omega^{k_s}$ the impedance again reduces to an equivalent damper with damping coefficient c_g, being

$$\omega^z = \frac{c_g}{J_g} = \frac{P_v I_t}{1 + P_t P_v}. \tag{22}$$

For $\omega > \omega^{k_s}$ the impedance of the physical spring is felt on the output shaft. In Fig. 4 the Bode plot of the frequency response $Z^z(j\omega)$ (calculated with numerical values reported in Tab. I) is reported, which shows the described features.

In order to further reduce the impedance, the gains should be possibly chosen so to increase ω^z, thus enlarging the inertial zone, which has a lower impedance magnitude. This can be achieved by increasing I_t, as shown in Fig. 5 where $\bar{Z}^z(j\omega) = Z^z(j\omega)|_{I_t = 2J_a{}^{-1}}$ is representatively reported. In this specific example the value of the torque control integral gain is set so that the apparent inertia is halved with respect to the physical one. It is also worth adding that the calculation of $Z^z(j\omega)$ is based on gains satisfying conditions in [14] while the calculation of $\bar{Z}^z(j\omega)$ is based on gains satisfying (4). It comes that conditions derived here can be considered less conservative and enable a larger reduction of the impedance magnitude. Therefore, viscous friction, in a sense, indirectly contributes to improve the active reduction of the output impedance: according to (4), for a selected value of the proportional gain P_v, the term ν (and hence I_t) can be increased with increasing c_a.

Considering (22), another solution to increase the frequency range in which pure inertia is displayed consists in decreasing the gain P_t. Anyhow, this solution has the drawback of increasing the parasitic damping c_g, according to (19), and of decreasing the torque control bandwidth.

Finally, null integrators would have implied a deviation from the desired impedance. Since

$$\lim_{s\to 0} Z^z(s)|_{\mu=\nu=0} = c_g + \frac{c_a}{P_t P_v + 1} := c^z, \tag{23}$$

at low frequencies the impedance would have reduced to the one of a pure damper with damping coefficient c^z, which depends not only on the controller gains but also from the intrinsic viscous friction.

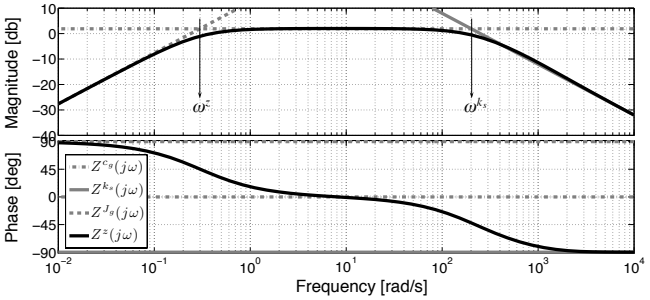

Fig. 4. Frequency response of the actuator impedance $Z^z(j\omega)$ in zero impedance mode. For frequencies below ω^z the actuator behaves like a pure inertia J_g ($Z^{J_g}(j\omega)$). For frequencies higher than ω^{k_s} the impedance reduces to the one of the physical spring ($Z^{k_s}(j\omega)$). For $\omega^z < \omega < \omega^{k_s}$ a damper, with coefficient c_g, is displayed (frequency response $Z^{c_g}(j\omega)$).

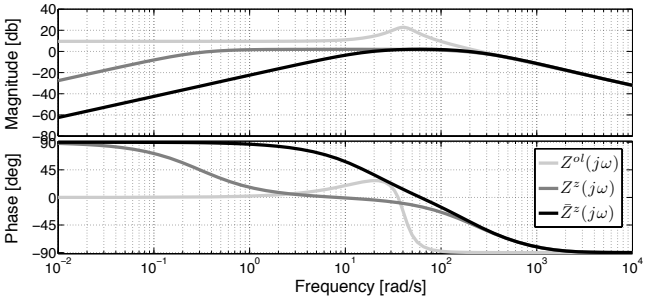

Fig. 5. Comparison among intrinsic impedance of the actuator ($Z^{ol}(j\omega)$), impedance calculated with gain values reported in Tab. I ($Z^z(j\omega)$) and impedance calculated with P_t reported in Tab. I and $I_t = 2J_a{}^{-1}$ ($\bar{Z}^z(j\omega)$).

V. Discussion and Conclusions

Torque control of SEAs is often implemented based on a PI control loop (exploiting the torque measurement provided by the series spring) that generates a set-point for a low-level PI velocity controller driving the motor. This cascade approach is often adopted for its effectiveness and ease of tuning/implementation and for its potential of guaranteeing passivity. To provide safe and comfortable physical interaction in human-centered applications, torque controlled SEAs can be employed to haptically display viscoelastic torques based on a third outer impedance control loop.

In this paper, the cascade controlled SEA was modeled and passivity for the rendering of a virtual parallel spring-damper system at the impedance control level was analyzed, thus generalizing results presented in [14], [15]. Two particular cases (pure elasticity and null impedance) were also considered. Guidelines for the design of the controller gains and the range of renderable virtual impedance were deduced.

When a parallel spring-damper system is rendered, passivity criterion cannot be satisfied. In particular, the Bode plot in Fig. 2 shows that $\angle Z^{sd}(j\omega) < -90$ deg only up to the frequency $\omega^{sd,p}$ estimated through (9) and if constraints (12) and (14) are taken into account in addition to (4). The virtual stiffness k can be linearly increased with the damping coefficient c, being the linear relation provided by the most conservative between (10) and (13), as shown by

(15). A spring with stiffness higher than the one of the series compliant element can be theoretically rendered, and can be increased with c, but stable interaction with any passive environments cannot be proved.

When a pure virtual spring is desired, according to (16) the maximum virtual stiffness is not only bounded by the value of the physical series spring, but by a value $\tilde{k}^s$, which depends on the controller gains and on the intrinsic viscous friction c_a and is independent of the inertia J_a. Since $\tilde{k}^s$ slightly decreases with c_a, stiffness control is robust against viscous friction variations. If a specific value of the virtual stiffness $\bar{k} = \alpha k_s$ has to be guaranteed in passive conditions, a gain tuning taking into account (17) is required: the increase of the torque control proportional gain P_t could not suffice and also velocity gains should be modified. The desired virtual elasticity is displayed up to the frequency ω^s, calculated with (18), while the output impedance approaches the one of the physical spring for high frequencies and of a damper with damping coefficient c_g, provided by (19) and only depending on the control gains, for intermediate frequencies.

In zero impedance mode, the conditions ensuring the stability of the low-level torque controller also guarantee passivity. Moreover, if no integrators are employed, the SEA is automatically passive but the impedance of the system reduces (for $\omega < \omega^{k_s}$) to a pure damper c_g, thus resulting in a potentially impeded retrograde motion. The PI-based cascade torque control can lower intrinsic friction (residual damping c_g can be easily made lower than c_a) without the need for a feedforward compensation approach. For low frequencies, the SEA displays a pure inertia J_g, which is inversely proportional to the torque control integral gain I_t. This behavior is achieved up to the frequency ω^z in (22), after which a damper c_g is again rendered. This parasitic damping effect can be reduced by increasing ω^z thus enlarging the bandwidth at which a pure inertia is rendered. This result can be obtained more conveniently by increasing I_t rather than by lowering P_t, in order to avoid the reduction of the torque control bandwidth. The constraints on gains selection proposed in [15] limit I_t, conversely, generalized conditions presented in this paper are less conservative and allow to further reduce the perceived impedance. Finally, it can be noticed that, for a fixed proportional velocity gain P_v, the increase of I_t is facilitated by the intrinsic friction according to (4).

In the analyzed cases, inequalities (4) have to be considered to satisfy passivity conditions described in Sec. II-B. Specifically, for a real prototype, (4) can be seen as constraints on the ratio between proportional and integral gains once fixed a value P_v compatible with saturation effects. When gains selection implies the knowledge of the viscous friction, a bounded variation of this value has to be ensured to allow robustness of the controller. Finally, the presence of integrators avoids deviations from the desired stiffness in both cases of parallel spring-damper and pure elasticity. In zero impedance mode it minimizes the parasitic damping effect which depends on the controller gains and on the intrinsic viscous friction. The presented theoretical results will be validated by using the SEA prototype described in [11] to investigate unmodeled features and possible unstabilities due to the lack of passivity during the interaction with passive environments and/or with human subjects.

REFERENCES

[1] N. L. Tagliamonte, F. Sergi, D. Accoto, G. Carpino, E. Guglielmelli, "Double actuation architectures for rendering variable impedance in compliant robots: A review," *Mechatronics*, vol. 22, no. 8, pp. 1187–1203, 2012.

[2] N. Hogan, "Impedance control: An approach to manipulation: Parts I, II, and III," *J Dyn Syst-T ASME*, vol. 107, pp. 1–24, 1985.

[3] G. Pratt and M. Williamson, "Series elastic actuators," *Int Conf Intelligent Robots and Systems*, vol. 1, pp. 399–406, 1995.

[4] D. Robinson, "Design and analysis of series elasticity in closed-loop actuator force control," *Ph.D. dissertation, MIT, Cambridge*, 2000.

[5] G. Carpino, D. Accoto, F. Sergi, N. L. Tagliamonte, and E. Guglielmelli, "A novel compact torsional spring for series elastic actuators for assistive wearable robots," *J Mech Design*, vol. 134, no. 12, 2012.

[6] D. Accoto, N. L. Tagliamonte, G. Carpino, F. Sergi, M. D. Palo, and E. Guglielmelli, "pVEJ: A modular passive viscoelastic joint for assistive wearable robots," *Int Conf Robotics and Automation*, pp. 3361–3366, 2012.

[7] J. F. Veneman, R. Ekkelenkamp, R. Kruidhof, F. van der Helm, and H. van der Kooij, "A Series Elastic- and Bowden-cable-based actuation system for use as torque actuator in exoskeleton-type robots," *Int J Robot Res*, vol. 25, no. 3, pp. 261–281, 2006.

[8] C. Lagoda, A. Schouten, A. Stienen, E. Hekman, and H. van der Kooij, "Design of an electric series elastic actuated joint for robotic gait rehabilitation training," *Int Conf Biomedical Robotics and Biomechatronics*, pp. 21–26, 2010.

[9] G. Wyeth, "Demonstrating the safety and performance of a velocity sourced series elastic actuator," *Int Conf Robotics and Automation*, pp. 3642–3647, 2008.

[10] F. Sergi, D. Accoto, G. Carpino, N. L. Tagliamonte, and E. Guglielmelli, "Design and characterization of a compact rotary series elastic actuator for knee assistance during overground walking," *Int Conf Biom Robotics and Biomechatronics*, pp. 1931–1936, 2012.

[11] D. Accoto, G. Carpino, F. Sergi, N. L. Tagliamonte, L. Zollo, and E. Guglielmelli, "Design and characterization of a novel high-power series elastic actuator for a lower limbs robotic orthosis," *Int J Adv Robot Syst*, vol. 10, 2013.

[12] K. Kong, J. Bae, and M. Tomizuka, "Control of rotary series elastic actuator for ideal force-mode actuation in human–robot interaction applications," *IEEE/ASME T Mech*, vol. 14, pp. 105–118, feb. 2009.

[13] N. L. Tagliamonte, F. Sergi, G. Carpino, D. Accoto, and E. Guglielmelli, "Human-robot interaction tests on a novel robot for gait assistance," *Int Conf Rehabilitation Robotics*, 2013.

[14] H. Vallery, R. Ekkelenkamp, H. van der Kooij, and M. Buss, "Passive and accurate torque control of series elastic actuators," *Int Conf Intelligent Robots and Systems*, pp. 3534–3538, 2007.

[15] H. Vallery, J. Veneman, E. van Asseldonk, R. Ekkelenkamp, M. Buss, and H. van der Kooij, "Compliant actuation of rehabilitation robots: benefits and limitations of series elastic actuators," *IEEE Robot Autom Mag*, vol. 15, no. 3, pp. 60–69, 2008.

[16] M. Grun, R. Muller, and U. Konigorski, "Model based control of series elastic actuators," *Int Conf Biomedical Robotics and Biomechatronics*, pp. 538–543, 2012.

[17] R. Ronsse, S. M. M. De Rossi, N. Vitiello, T. Lenzi, M. C. Carrozza, A. J. Ijspeert, "Real-Time Estimate of Velocity and Acceleration of Quasi-Periodic Signals Using Adaptive Oscillators," *IEEE Trans Robot*, vol. 29, pp. 783–791, 2013.

[18] E. Colgate and N. Hogan, "An analysis of contact instability in terms of passive physical equivalents," *Int Conf Robotics and Automation*, pp. 404–409 vol.1, 1989.

[19] J. E. Colgate, "The control of dynamically interacting systems," *Ph.D. dissertation, MIT, Cambridge*, 1988.

[20] S. P. Buerger and N. Hogan, "Complementary Stability and Loop Shaping for Improved Human-Robot Interaction," *IEEE Trans Robot*, pp. 232–244, 2007.

[21] N. L. Tagliamonte, M. Scorcia, D. Formica, D. Campolo, and E. Guglielmelli, "Effects of impedance reduction of a robot for wrist rehabilitation on human motor strategies in healthy subjects during pointing tasks," *Adv Robot*, vol. 25, pp. 537–562, 2011.